CO_2 electro/photocatalytic reduction using nanostructured ZnO and silicon-based materials: A short review

Article history:
Received: 21-01-2023
Revised: 18-04-2023
Accepted: 20-05-2023

Andrés Galdámez-Martínez[a], Ateet Dutt[b]

Abstract: Reducing CO_2 net emissions is one of the most pressing goals in tackling the current global warming emergency. Therefore, the development of carbon recycling strategies has resulted in the application of heterogeneous catalysts toward the electro/photocatalysis reduction of CO_2 into hydrocarbons with potential reusability.Their morphology affects the performance and selectivity of catalysts toward this reaction. Nanostructuring methods offer popular strategies for catalytic applications since they allow an increase in the area/volume ratio and versatile control over surface physicochemical properties. In this review, we summarize studies that report the use of versatile synthesis techniques for obtaining nanostructured metallic and semiconductor materials with application in the electro/photocatalytic reduction of CO_2. Enhancing mechanisms to the catalytic CO_2 reduction yield, such as improved charge carrier separation efficiency, defect engineering, active site concentration, and localized plasmonic behavior,are described in conjunction with the control over the morphologies of the nanostructured platforms. Special attention is given to ZnO and silicon-based matrices as candidates for developing abundant and non-toxic catalytic materials. Therefore, this work represents a guide to the efforts made to design electro/photocatalytic systems that can contribute significantly to this field.

Keywords: CO_2 reduction; carbon recycling; electro/photocatalysis; ZnO nanostructures .

Introduction

As the world grapples with the devastating impacts of climate change, sustainable technologies are needed to reduce greenhouse gas emissions. Carbon dioxide (CO_2) is one of the most abundant greenhouse gases. Its conversion to valuable and value-added products such as fuels and chemicals is a promising approach for mitigating its adverse effects (D. Li *et al.*, 2020). This process can be achieved through various methods such as electrocatalytic, photocatalytic, and electro/photocatalytic CO_2 reduction (J. He *et al.*, 2018; Shehzad *et al.*, 2018).

Semiconducting materials are ideal for electrocatalytic CO_2 reduction due to their ability to catalyze the reaction at the electrode interface (J. He *et al.*, 2018). In photocatalytic CO_2 reduction, semiconducting materials are excited by light energy to generate electrons and holes, which can drive the CO_2 reduction reaction (Shehzad *et al.*, 2018). The electro/photocatalytic approach combines the electrocatalytic and photocatalytic approaches by using an electrode to supply an external potential to the photocatalyst and enhance its activity (Chen *et al.*, 2021).

[a] Instituto de Investigaciones en Materiales Universidad Nacional Autónoma de México, México City, México.
Equal Contribution.

[b] Instituto de Investigaciones en Materiales Universidad Nacional Autónoma de México, México City, México.
Equal Contribution.
adutt@iim.unam.mx
Corresponding author.

https://doi.org/10.37819/nanofab.8.306

Using semiconducting nanostructured materials in CO_2 reduction applications has shown significant potential for improving reaction efficiency and selectivity (Y. Wang *et al.*, 2021). Nanostructuring enhances the surface area and reduces the distance for charge carriers to travel, thus improving their catalytic yields. Various semiconducting materials such as tin sulfide (SnS_2), iron oxide (Fe_2O_3), tungsten oxide (WO_3), silicon carbide (SiC), bismuth oxide (BiO_2), titanium dioxide (TiO_2), zinc oxide (ZnO), and silicon (Si) have been used in the form of nanoparticles, nanowires, nanorods, and other nanostructures for CO_2 reduction applications (Habisreutinger *et al.*, 2013; Han *et al.*, 2020; L. Zhang *et al.*, 2017). However, the stability under harsh reaction conditions, reusability, and cost-effectiveness of semiconducting nanostructured materials in CO_2 reduction applications remain challenging (Shehzad *et al.*, 2018).

ZnO and Si are widely used materials in these approaches because of their tunable band gap, high electron mobility, and abundant availability. ZnO has a wide bandgap (3.37 eV) and a high exciton binding energy, making it an ideal material for photocatalytic applications under different reaction conditions (Galdámez-Martínez *et al.*, 2020). In addition, its low cost, abundance, and nontoxicity make it a promising alternative to other semiconductor materials. Si has high electron mobility, high conductivity, and good stability, making it suitable for photocatalytic applications (Wong *et al.*, 2017). At the same time, ZnO and Si nanomaterials have been demonstrated to be effective in CO_2 reduction using electrocatalytic, photocatalytic, and electro/photocatalytic approaches. ZnO and Si nanomaterials also exhibit versatile compatibility with other enhancing strategies, such as high aspect ratio ZnO nanorods and high surface area Si nanowires(F. Liao *et al.*, 2022). Furthermore, ZnO and Si nanomaterials have been coupled with various catalysts such as metal nanoparticles, metal oxides, and organic molecules to enhance CO_2 reduction performance (Ma *et al.*, 2021; X. Wang *et al.*, 2019).

This article aims to provide an overview of recent progress made in electrocatalytic, photocatalytic, and electro/photocatalytic CO_2 reduction using semiconducting nanostructured materials, focusing on ZnO and Si. The article will discuss the morphological and size-related effects of diverse nanomaterials over catalytic CO_2 reduction for mitigating climate change, as well as properties and synthesis methods for obtaining efficient ZnO and Si nanostructured catalyst materials for CO_2 carbon recycling. The strategies to improve the selectivity and activity of ZnO and Si nanostructured materials will also be addressed. This article will provide an understanding of the progress made in this field and highlights the challenges and opportunities for future research.

Morphological and size dependence of electro/photocatalytic reduction of Co_2

Semiconducting compounds, metal oxides, chalcogenides, and metals such as TiO_2, Fe_2O_3, WO_3, ZrO_2, Cu, Co, Au, SnS_2, SiC, BiO_2, and ZnO have been used for the photocatalytic and photoelectrocatalytic reduction of CO_2 (Feng *et al.*, 2022; Z. H. Gao *et al.*, 2022; Qiao *et al.*, 2022; Woldu *et al.*, 2022). Inoue *et al.* (1979) reported the use of TiO_2, ZnO, CdS, GaP, SiC, and WO_3 powders as photoelectrocatalytic materials for obtaining organic fuels (e.g., formic acid: CH_2O_2, formaldehyde: CH_2O, methanol: CH_4O, and methane: CH_4) through a CO_2 reduction process. Since then, these compounds have been widely implemented in such applications (H. Li *et al.*, 2011; N. Li *et al.*, 2022; Loutzenhiser *et al.*, 2010; G. Yang *et al.*, 2022; X. Zhang *et al.*, 2022).

Although the effect of some parameters, such as pH and temperature,over the electro/photocatalytic performance toward the reduction of CO_2 has been studied in the past (de Brito *et al.*, 2015; Zhao *et al.*, 2012), the role of the catalyst morphological properties is yet to be discussed. Control over the morphology of the nanostructures has been and continues to be an actual goal within the science of materials, therefore parameters such as particle diameter, pore size, aspect ratio, sphericity, rugosity, and dimensionality, among others, can be tuned using multiple synthesis techniques, as it can be seen in Table 1.

For instance, in the work of Rong *et al.* (2021), the size effect of Cu nanoclusters on the electrocatalytic reduction of CO_2 is presented. The authors use an acetylenic-bond-directed site-trapping method to synthesizeCu nanoclusters (0.5-1.5 nm range) immersed in a graphdiyne matrix. The response of the catalytic system shows an increase (both in selectivity and activity) towards multicarbon products (C_{2+}) as the size of the nanoclusters rises. This catalytic enhancing effect is attributed to a higher number of surface atoms with low coordination numbers. Also, the metallic composite demonstrates good stability due to Cu-C bonds. The electrocatalytic system reports a Faradic Efficiency (FE) of 94% towards C_{2+} products using −0.8V with respect to a reversible hydrogen electrode (RHE).

Material	Type of platform	Morphological parameters	Enhancing effect	Synthesis technique	Yield/Rate	Product	Ref
Cu nanoclusters on GDY matrix	Electrocatalytic	s=0.5-1.5 nm	Low-coordinated atoms in the surface	Acetylenic-bond-directed site-trapping method	312 mA cm^{-2}	Multicarbon products	(Rong *et al.*, 2021)
In_xCu_yNPs	Electrocatalytic	d=5-15 nm	Decrease of formic acid reduction potential	Citrate reduction technique	90% FE at −1.2 V vs. RHE	CH_2O_2	(Wei *et al.*, 2021)
Co@ZIF composite	Electrocatalytic	s=6-18 nm	Larger surface area	Chemical reduction and pyrolysis treatment	4.2 mA cm^{-2}	CO	(Miao *et al.*, 2020)
Ni@ZIF composite	Electrocatalytic	s=4-37 nm	Lower energy formation of CHO_2 using smaller NPs	Chemical reduction and pyrolysis treatment	95% FE at −0.8 V vs. RHE	CO	(Z. Li *et al.*, 2020)
F-SnS_2 and T-SnS_2	Photocatalytic	s(F–SnS_2)=10 nm/s (T–SnS_2) 80-120 nm	Improved charge separation	Hydrothermal method	97.5 μmol g^{-1}	CO, CH_4	(G. Li *et al.*, 2020)
Cu NWs	Electrocatalytic	l=2.9-13.4 μm d=50-100 nm	Larger surface area and defect engineering	Thermally and electrochemically reduced	30% FE at −0.5 V vs. RHE	CO	(Y. Wang *et al.*, 2020)
Ni foam/ZnO photocatode	Photoelectro-catalytic	—	C-C coupling and efficient charge transport	Electrochemical deposition	3.75 μM h^{-1} cm^{-2} / 10 μM h^{-1} cm^{-2}	$C_2H_4O_2$/ C_2H_6O	(J. Wang *et al.*, 2018)
Bi nanosheets	Electroreduction	t=10 nm	A high density of active sites on (102) Bi facet	Hydrothermal method	85% FE at −0.85 V vs. RHE	CHO_2^-	(T. Gao *et al.*, 2019)
Ag-CeO_2 composite	Photocatalytic	ps=4.8-31.8 nm	Enhanced SPR and Schottky barrier formation	Hydrothermal method	100 μmol h^{-1}/ 35 μmol h^{-1}	CH_4/ CH_4O	(Cai *et al.*, 2018)
TiO_2 NPs	Photocatalytic	d=4.5-29 nm	Larger surface area, charge transport, and improved light absorption	Sol-Gel method	0.16 μmol m^{-2} / 0.02 μmol m^{-2}	CH_4/ CH_4O	(Kočí *et al.*, 2009)
MOF/Cr–Ag NPs	Photocatalytic	d=80-800nm	Efficient charge transport	Chemical bath	808.2 μmol $g^{-1}h^{-1}$ / 427.5 μmol $g^{-1}h^{-1}$	CO / CH_4	(F. Guo *et al.*, 2019)
Black TiO_2@ Silica PNPs	Photocatalytic	d=1-12 nm	Highly accessible surface, efficient charge transport, and separation	Hydrogen thermal reduction	14.7 μmol g^{-1} h^{-1} / 124.3 μmol g^{-1} h^{-1}	CO / CH_4	(Xuan *et al.*, 2019)
Pd-Cu nanocatalyst	Electroreduction	d=16-20 nm	Low-coordinated atoms in the surface	Chemical bath	40.6% FE at −1.2 V vs. RHE	CH_4	(Zhu *et al.*, 2018)

*GDY: graphdiyne; ZIF: zeolitic imidazolate frameworks; T-SnS_2: Tablet-like SnS_2 nanostructure; F-SnS_2: Flower-like SnS_2 nanostructure; SPR: surface plasmon resonance; MOF: metalorganic framework; PNPs: porous nanoparticles; size: s; diameter: d; length: l; thickness: t; ps: pore size.

Table 1. Different nanostructured morphologies implementation to CO_2 electro/photocatalytic reduction.

Another electrocatalytic study is presented by the research group of Wei *et al.* (2021), where the implementation of bimetallic indium-copper (In_x-Cu_y) nanoparticles (NPs) with controlled crystallographic facets for the CO_2 reduction to formic acid is presented. Tunning theCu to In ratio led to the obtention of controlled In_xCu_y (x and $y = 3.0$-0.5 range) NPs through a citrate reduction technique. The technique also allows control over the growth direction of the structure.The authors' DFT calculations suggested that the (101) facet of In is indeed desired for the production of CH_2O_2 due to a decrease in the formic acid reduction potential with respect to this particular crystal face. The authors report a FE of 90% towards CH_2O_2 at −1.2 eV vs. RHE using $In_{1.5}Cu_{0.5}$.

On the other hand, the size variation of Co nanoparticles in a zeolitic imidazolate framework (Zn-Co@N-C) and their effect on the electroreduction of CO_2 were studied by Miao *et al.* (2020). The chemical reduction approach used by this research team allows the obtentionof Co nanoparticles with a size distribution between 6 and 18 nm. An increment tendency in the catalytic performance with Co NPs-size reduction was also observed. This was mainly attributed to an increase in the system's surface area and to the presence of carbon layers coating the metal nanoparticles through a prior pyrolysis treatment in a nitrogen atmosphere. As a result, they report a reduction rate of 4.2 mA cm^{-2} towards carbon monoxide (CO) using the Zn-Co@N-C nanocomposite. The system presented a stable electrocatalytic efficiency activity for up to 40 h, making it a promising candidate for this application. Other works referring to size-related effects of the catalyst material on the carbon dioxide reduction performance can be found in Table 1.

Furthermore, some authors have explored the morphological properties of semiconducting materials over the photoreduction of CO_2, as found in Sun *et al.*'s work (G. Li *et al.*, 2020). By conducting comparative tests to obtain CO and CH_4 as products of photocatalytic carbon dioxide reduction, the performance and stability of SnS_2 nanostructures with different morphologies and dimensions were evaluated. Therefore, tablet-like and flower-like SnS_2 nanostructures (80-120 and 10 nm in size, respectively) were obtained by a hydrothermal method.The results showed a better charge separation effect in smaller catalysts, thus obtaining an improved reduction rate of 97.5 μmol g^{-1} towards CH_4 for flower-like structures.

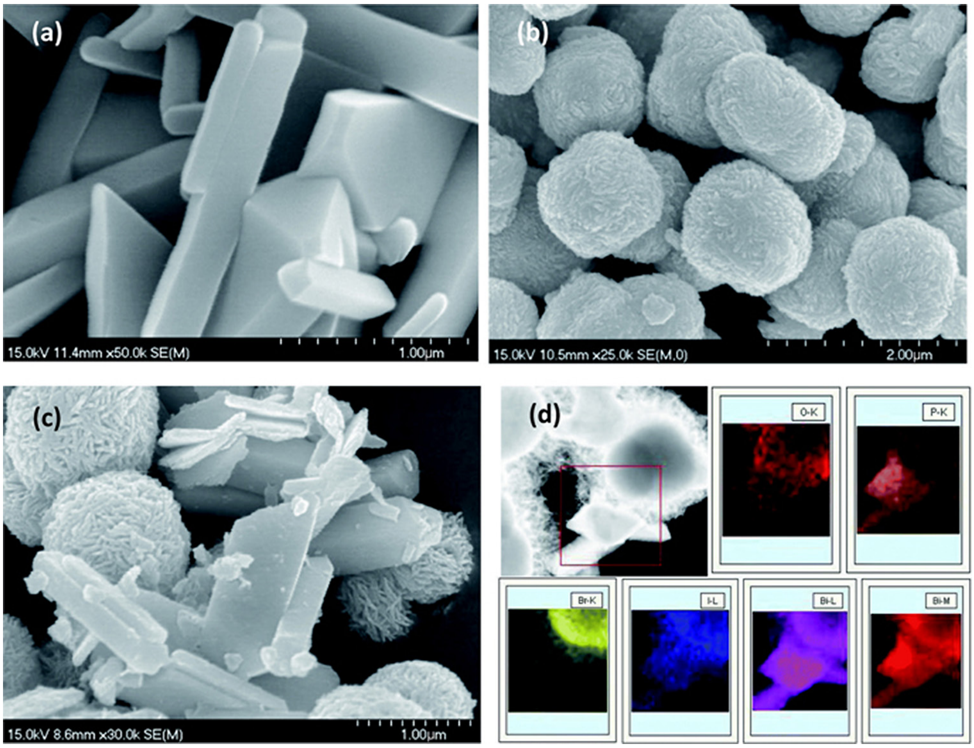

Figure 1. Formation of $BiPO_4$-$BiOBr_{0.75}I_{0.25}$ composites by solvothermal technique for photocatalytic CO_2 reduction. (a) $BiPO_4$ crystals, (b) $BiOBr_{0.75}I_{0.25}$ spheres, (c) heterojunction, (d) EDX mapping (Yin *et al.*, 2019). Copyrights RSC 2019.

On the other hand, Yin *et al.* (2019) showed successful band structure modulation of morphologically controlled semiconductor materials for photocatalytic CO_2 reduction. In this study, the authors describe a solvothermal synthesis of n-p composites ($BiPO_4$-$BiOBr_{0.75}I_{0.25}$). Figure 1 depicts the SEM images of $BiPO_4$ (a), $BiOBr_{0.75}I_{0.25}$ (b), and the integration of both systems (c) with their corresponding EDX mappings (d). Under visible light irradiation (>420 nm) of 1900 mW cm^{-2}, the composite exhibited a CO production of 24.9 µmol g^{-1} and a CH_4 yield of 9.4 µmol g^{-1}, larger than that of the individual semiconductors. In addition to the increase in the surface area owing to the reduction in particle size, the effective carrier separation due to heterojunction is postulated as the primary mechanism for enhancing the platform's catalytic performance. In addition, the authors claim that the relative concentration of I and Br permits control over the band structure of the heterojunction, hence allowing the system to be applied to other photocatalytic reactions.

Although much of the literature reports the use of zero-dimensional (0D) nanostructures, the implementation of one-dimensional (1D) Cu nanostructures (i.e., nanowires: NWs) for the electroreduction of CO_2 is stepped up by Yuanxing Wang *et al.* (2020). The Cu NWs were obtained either by an electrochemically or thermally reduction approach of CuO NWs.The obtained nanostructures present lengths and diameters in the 2.9-13.4 µm and 50-100 nm range, respectively. Either increasing the nanowire length or raising the defect density along the nanostructure led to a higher FE. As the thermal reduction process was carried out in a controlled atmosphere, the surface defects of the nanowire can be engineeredto improve the selectivity of the CO_2 reduction.

In addition, the use of different morphologies of ZnO/Ni electrodes in a photoelectrocatalytic cell for the CO_2 reduction to acetic acid is performed by J. Wang *et al.* (2018). A photoelectrocatalytic cell was designed using $BiVO_4$ as photoanode material and electrochemically deposited ZnO/Ni as a photocathode. Diverse ZnO/Ni composite morphologies such as porous nanoparticles, ball cactus, and nanorods were achieved by controlling the deposition time. The catalytic rates were found to be 3.75 µM h^{-1} cm^{-2} toward acetic acid and 10 µM h^{-1} cm^{-2} for ethanol, both using nanorod-like structures. Then it is suggested that this morphology offers optimum surface disponibility and an efficient charge transfer phenomenon.

Moreover, T. Gao *et al.* (2019) report using different Bi nanostructured morphologies, including nanowires, nanospheres, and nanosheets for CO_2 electroreduction to CHO_2^- finding a better performance for the bi-dimensional (2D) morphology. According to the authors, this is primarily due to the high presence of (012) facets which present more active sites for the catalytic reaction. The nanosheets offer good stability in 8h tests and FE of 85% to formate at −0.85 V vs. RHE.

Therefore, it is possible to affirm that those nanoengineering processes that allow precise control over the morphological properties can be implemented to design the next generation of catalytic materials to reduce CO_2.

However, many authors have reported important obstacles to overcome for these compounds to work as efficient electro/photocatalytic materials. Good catalytic activity, as well as durability, stability, and resistance to photo corrosion in aqueous media, are among the main goals to be achieved. For example, the low stability of chalcogenide compounds (e.g., CdS, CdSe) in heterogeneous photocatalysis reactions imposes the use of additional agents (e.g., sulfide, sulfite) that suppress the photo corrosion of the photoactive compound (Kočí *et al.*, 2017; C. Wang *et al.*, 2011). In this sense, materials such as ZnO and Si that meet the above-mentioned requirements and stand out for their morphological versatilitydisplay promising potential forcatalytic CO_2 reduction applications.

ZnO-based photocatalytic and photoelectrocatalytic reduction of CO_2

Despite their large bandgap values that make their photoexcitation process UV-dependent, TiO_2, and ZnO present a photocatalytic performance higher than some visible excitable photocatalysts due to their inherent surface stability (Fox & Dulay, 1993). In the case of titanium dioxide, its crystal structures (rutile, anatase, and brookite) have been used in the photocatalytic reduction of CO_2. According to Bouras *et al.* (2007), combining anatase with a slight amount of rutile produces optimal photocatalytic efficiency.However, effectivecharge transport, rapid recombination of photoexcited electrons and holes, limited selectivity, and high surface energy are among the main limitations of TiO_2 in photocatalytic reactions (Dong *et al.*, 2015). In thisregard, ZnO displays anelectron mobility 10-100 times greater than TiO_2 (Jayah *et* *al.*, 2015) which makes it a suitable candidate in photocatalysis as photogenerated charge carriers can rapidly reach the surface of the material, diminishing the recombination losses. ZnO is an II–VI semiconductor with a near UV direct bandgap (Galdámez-Martínez *et al.*, 2020). It is also a cheap, abundant, non-toxic material with good stability. As a photocatalyst, it has a suitable band structure meeting the thermodynamic requirement for CO_2 photoreduction due to sufficient reductive power of its conduction band (CB ≈ −0.31 vs.NHE at pH 7) and also for water oxidation owing to its valence band position (VB ≈ 2.91 V vs. NHE at pH 7) (W.-N. Wang *et al.*, 2014).

The photoreduction of carbon dioxide to methanol using ZnO under visible light was studied by Watanabe *et al.* (1992). In this work, the photocatalytic activity of the system in the visible spectra (even though it should only be active in the UV region) is attributed to the presence of surface levels result of S, Si, and P impurities. The experiment was carried out in a high-pressure atmosphere of CO_2 using ZnO powder in aqueous media. Comparing the photoreduction performance of $SrTiO_3$, TiO_2, and ZnO under the same high-pressure conditions resulted in ZnO displaying a higher catalytic yield toward methanol and methane, with an estimated efficiency of 6% (calculated with respect to the number of reactant H_2O molecules).

Núñez *et al.* (2013) studied the photoreduction of CO_2 to CO, H_2, CH_4, and CH_4O as main products in the presence of N- and Cu-doped mesoporous ZnO structure and using H_2O in the gas phase as reductant. In this work, the morphological and chemical modifications improve the photocatalytic properties of ZnO. As expected, incorporating N atoms into the ZnO structure produced changes in the material's band structure, enhancing its visible photoexcitation. However, the best results were obtained with the mesoporous structure's synergywith the addition of copper as a co-catalyst. The improved textural properties of the porous semiconductor matrix favored the dispersion and interaction with the cooper centers resulting in a decrease of the electrons-holes recombination rate.

Photocatalytic reduction of CO_2 to CH_4O using zinc oxide/reduced graphene oxide nanocomposites (ZnO–rGO) has been reported by Lixin Zhang *et al.* (2015). The implementation of ZnO–rGO structures has been widely reported by other authors as well (Ali *et al.*, 2018; Deng *et al.*, 2020; L. Liu & Jin, 2017; Xu *et al.*, 2018; Zheng *et al.*, 2018) as a strategy to enhance electron transport efficiency and decrease the recombination of electron-hole pairs in ZnO. In the work of Zhang, the incorporation of reduced graphite oxide into the ZnO nanoparticle (5-25 nm) results in a five times higher methanol yield than pure ZnO. The reported CO yield for each of the employed morphologies was: nanorod (3.814 μmol g^{-1} h^{-1}) in comparison with ZnO microspheres (3.357 μmol g^{-1} h^{-1}) and microflowers (1.627 μmol g^{-1} h^{-1}).

Y. Liao *et al.* (2015) used a biofunctionalized ZnO structure to get a better photocatalytic CO_2 reduction. ZnO nanosheets obtained by the hydrothermal method were amine-functionalized to get better chemisorption properties. Therefore, the CO_2 photoreduction on the semiconductor-activatedsurface was enhanced.

Furthermore, X. Jiang *et al.* (2016) made an efficient catalytic system for the electroreduction of CO_2. ZnO nanoporous structures were prepared by hydrothermal technique followed by a thermal decomposition process to reduce the material's surface to Zn. As expected, the reduced surface presents a higher FE and a better current density for CO generation than commercial Zn foils. The authors attribute the enhancement in the CO current density to the higher surface area presented by the nanoporous structure. Other authors have recently reported successful electroreduction of CO_2 using ZnO-based materials (Basumallick, 2020; Geng *et al.*, 2018; Ghahramanifard *et al.*, 2018; K. Jiang *et al.*, 2017; Merino-Garcia *et al.*, 2019).

Surface modification using Ce and La on the surface of ZnO was investigated by Q. Guo *et al.* (2017) for the efficient photoconversion of CO_2 to methane and methanol. Their study reveals that the appropriate presence of CeO_2 can improve CO_2 adsorption by forming an intermediate specie and increasing four times the CH_4 yield. The photoconversion was carried out using a 450 W Xe lamp in the UV-visible range (λ = 320-780 nm).

Oxygen deficient (ZnO_{1-x}) /carbon dots composites were used by Lin *et al.* (2018) for the photoreduction of carbon dioxide over the whole visible spectrum and even the UV and NIR regions. The heterostructures were obtained through asingle-step aerosol method. The synthesized system presents a significantly enhanced absorption in the hole UV–visible–NIR spectrum (300-1400 nm) due to absorbed energy by the ZnO matrix from up-converted emissions (410-560 nm) of the carbon dots. Also, a systematic analysis of the effect of the components' ratios over the material's physiochemical adsorption properties was performed to maximize the CO yield. The best CO production reported was 60.77 μmol g^{-1} h^{-1}, which is higher than that of pristine ZnO.

X. Wang *et al.* (2019) used a Fe_2O_3-ZnOrod/rGO heterostructure for the photocatalytic reduction of CO_2 with visible light illumination. An electrochemical growth was implemented to obtain the heterostructures. First, an aqueous solution of zinc powder and graphene oxide sheets (previously prepared by the Hummer method) was left under magnetic stirring for 40 min to produce Zn/rGO precipitate. Then, ferrous chloride was added to the solution. The mixture is finally taken to an electrochemical cell for the electrochemical growth of the ZnO microstructure. The introduction of the Fe_2O_3-ZnO/rGO heterojunction significantly lowered the electron-hole recombination rate. Furthermore, as reduced graphene oxide nanosheets presenthigh carrier transport features, they improve the catalytic efficiency of the system.

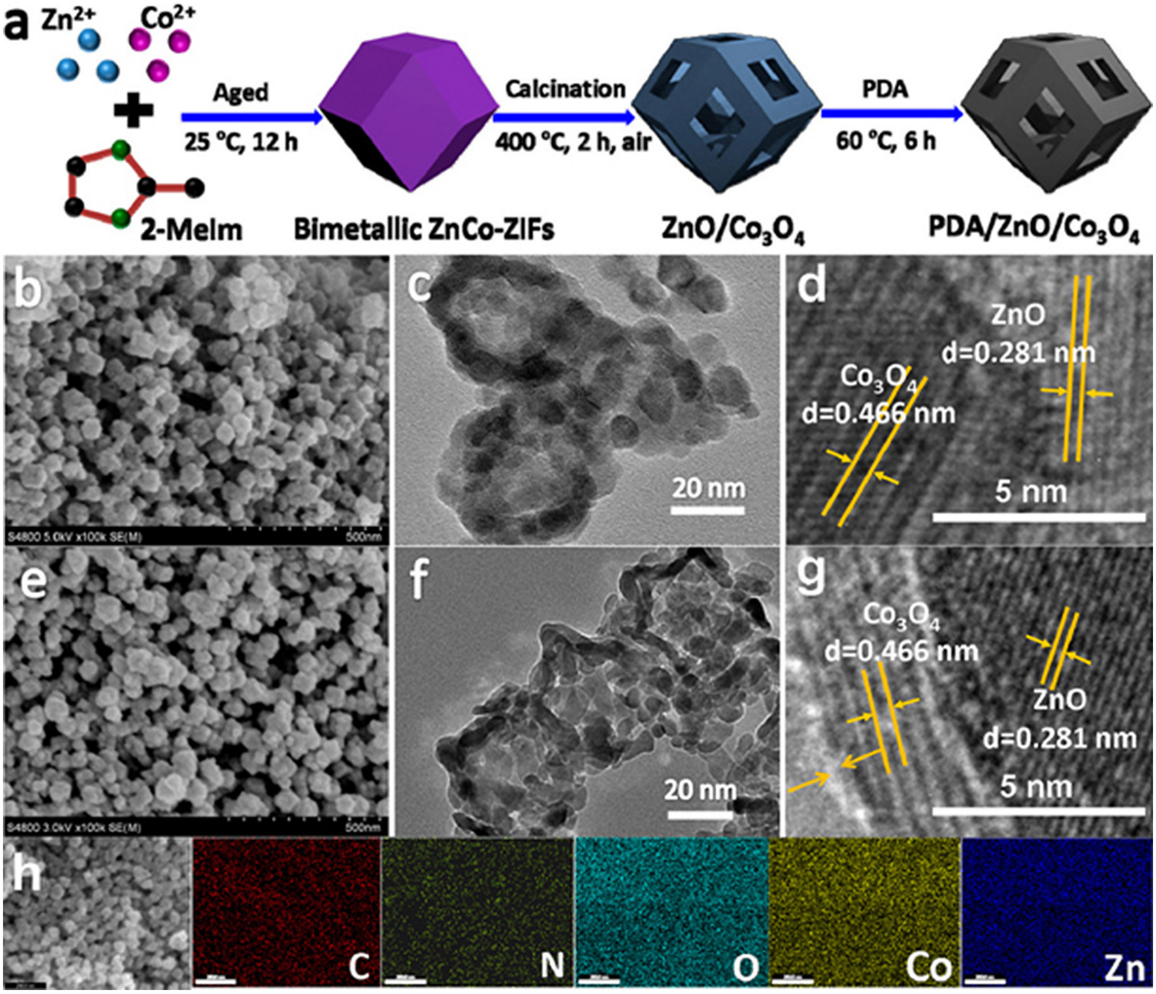

Figure 2. (a) Schematic representation of the synthesis process of ZnO/Co_3O_4 hollow bimetallic particles coated with polydopamine (PDA) for the photocatalytic reduction of CO_2. (b-d) ZnO/Co_3O_4 hollow particles obtained from the calcination of bimetallic zeolitic imidazolate frameworks. (f and g) Coating of the photocatalyst with PDA. (h) EDX mappings (M. Li *et al.*, 2020).Copyrights ACS 2020.

On the other hand, M. Li *et al.* (2020) presents the obtaining of hollow nanostructured photocatalysts composed of ZnO/Co_3O_4 heterojunctions for CO_2 reduction.The authors describe the calcination of Zn–Co zeolitic imidazolate frameworks (ZIFs) to formthe structures, as shown in Figure 2 (b-d). Afterward, the frameworks were coated with polydopamine (PDA) using a chemical bath (Figure 2 (e-g)) then to evaluate the photocatalytic performance for CO_2 reduction to CO, ensuing evolution of 537.5 μmol g^{-1} h^{-1} under a Xe (300W) lamp.As a result of the heterojunction created between the semiconductors, the authors demonstrate that the hollow porous structures present an effective charge separation and an outstanding selectivity towards CO (~98%) because of the PDA modification.

Finally, a study by Zhao *et al.* (2019) proposes usinga non-polar ZnO graphene-like structure (g-ZnO) for the efficient photoreduction of CO_2. They found out that when the thickness of the ZnO structure is reduced to a few monolayers, the adsorption of CO_2 is increased. A critical point is reached around 7-8 layers when competition between the further adsorption of carbon monoxide and the structural reconstruction of the system occurs. These ultrathin ZnO films present a band edge position fit for the CO_2 reduction to CH_4O and CH_4. The photocatalytic activity of these ZnO ultrathin films is attributed to the charge distribution and electron accumulation on the semiconductor surfaces. However, the promising feature of this work is that the concept of interlayer coupling a few monolayers and taking advantage of the quantum confinement effect can be applied to other metal oxides and semiconductors systems.

In Table 2, we present a summary of relevant literature on CO_2 photoreduction and electroreduction using ZnO structures.

Si-based photocatalytic and photoelectrocatalytic reduction of CO_2

Besides ZnO, other semiconductors, such as silicon, have also been used for the photo/electrocatalytic reduction of CO_2. The photocatalytic reduction of carbon dioxide to CH_2O_2, CH_2O, CH_4O, C_2H_4O, C_2H_6O using metal-loaded SiC powders is reported in the work of Yamamura *et al.* (1988). The 1000 mesh SiC powder was loaded with Pb, Cu, Pd, Fe, and Pt by mixing the components in a solution and then dried at 500 °C. It was found that metal-loading enhances the photocatalytic reduction of carbon dioxide, especially when Pd was added.

Shioya *et al.* (2003) reported the photocatalytic reduction of carbon dioxide to CH_4 and CH_4O using mesoporous silica thin films with tetrahedrally coordinated Ti ions embedded in the matrix. The films were obtained by using solvent evaporation, a method that not only allows control over the coordination of Ti species (tetrahedrally/octahedrally coordinated) but also over the geometry of the pores (cubic and hexagonal). The photocatalytic CO_2 reduction performance was evaluated using UV irradiation from a 100 W high-pressure Hg lamp. As expected, the yield of methane and methanol increased as irradiation time raised; however, a better catalytic activity was found in hexagonal pore structure films. Furthermore, the presence of OH groups on the surface of the materialled to a selective formation of CH_4O.

The photoassisted electrochemical performance of hydrogen-terminated p-type silicon photocathode for the reduction of CO_2 was reported by Kumar *et al.* (2010). A rhenium catalyst with bipyridine ligands (Re(bipy-Bu^t)$(CO)_3$Cl (bipy-But=4,4′-di-tert-butyl-2,2′-bipyridine) was used as an electrocatalyst for the selective photoreduction of CO_2 to CO. Even though the conduction band of p-type silicon is below the desired redox potentials, the reduction is feasible due to a charge transfer phenomenon known as Fermi-level pinning/unpinned band edges (Bocarsly *et al.*, 1980). Taking advantage of this feature, the p-type silicon photocathode reduction process could be achieved using a 600 mV lower potentialthan the one necessary forthe Pt electrode. Under a monochromatic illumination of 95 mW cm^{-2}, an overall conversion efficiency of 9.0% was reported.

O'Brien *et al.* (2014) synthesized ruthenium sputtered Si nanowires (Ru/SiNW) by using the metal-assisted chemical etching (MaCE) technique and study their use in the effective methanation of carbon dioxide in a hydrogen-rich environment(-Figure 3). The reaction by which carbon dioxide reacts (generally at high temperatures and pressures in the presence of a catalyst) to produce methane and water is known as the Sabatier reaction. The authors report that introducing the heterostructure thermochemically and photochemically favors the Sabatier reaction process.

According to them, this is due to the effect of localized heating or plasmons on the surface of the Ru particles surface (Christopher *et al.*, 2011), as well as favorable electronic polarity produced by photogenerated electron-hole pairs (Scirè *et al.*, 1998).

Photocatalyst	Enhancement	Synthesis	Light source	Reductant	Products	Yield	Ref
ZnO	—	—	75W Xe lamp $\lambda>398$ nm	H_2O	CH_4O	~ 6%*	(Watanabe, 1992)
Cu-Mesopouros ZnO	Doping /nanostructuration / cocatalyst	Hydrothermal method	8 W fluorescent lamp $\lambda_{max} = 369$ nm	H_2O	CO	CO 0.73 μmol g^{-1} h^{-1}	(Núñez *et al.*, 2013)
ZnO-reduced graphene oxide	Nanocomposite	Hydrothermal method	300 W Xe lamp	1.0 M NaOH solution	CH_4O	263.17 μmol g^{-1}	(L. Zhang *et al.*, 2015)
Cu_2O-ZnO nanorods	Nanocomposite	Electrodeposition	300 W Xe lamp	0.25 M Na_2SO_3 /1.0 M NaOH solution	CO	—	(Iqbal *et al.*, 2018)
Amine-functionalized ZnO nanosheets	Sensitization	Hydrothermal method	Xe lamp	H_2O	H_2, O_2, CO, CH_4	H_2 (81 ppm), O_2 (1145 ppm), CO (1520 ppm), CH_4 (146 ppm)	(Iqbal *et al.*, 2018)
ZnO microspheres, microflowers, and nanorods	Nanostructuration	Solvothermal method	300 W Xe lamp	H_2O	CO	Nanorod (3.814 μmol g^{-1} h^{-1}) microspheres (3.357 μmol g^{-1} h^{-1}) microflowers (1.627 μmol g^{-1} h^{-1})	(X. Liu *et al.*, 2016)
Reduced nanoporous ZnO	Nanostructuration/surface modification	Hydrothermal method	Autolab potentiostat	0.25 M K_2SO_4 solution	CO	CO current density 15.1 mA cm^{-2}	(X. Jiang *et al.*, 2016)
La-Ce co-modified ZnO nanorod	Rare earth doping	Hydrothermal method	450 W Xe lamp (λ= 320-780 nm	H_2O	CH_4, CH_4O	CH_4 26.8 μmol g^{-1} CH_4O 40.7 μmol g^{-1}	(Q. Guo *et al.*, 2017)
ZnO_{1-x}/carbon dots	Heterostructure	Single-step aerosol process	UV-vis-NIR (300-1400 nm)	H_2O	CO	60.77 μmol g^{-1} h^{-1}	(Lin *et al.*, 2018)
α-Fe_2O_3-ZnO rod/(rGO)	Heterostructure	Redox replacement and electrochemical growth	300 W Xe lamp ($\lambda>420$ nm)	H_2O	CH_4O	9.7 μmol g^{-1}	(X. Wang *et al.*, 2019)
Porous ZnO nanoplates	Nanostructuration/surface modification	Solvothermal method	300 W Xe lamp	H_2O	CO	3.8 μmol g^{-1}	(P. Li *et al.*, 2019)

Table 2. ZnO systems used for CO_2 photo/electro reduction.

The methanation process was carried out in a hydrogen atmosphere of a mixture of H_2:CO_2 gases at a ratio of 4:1. The methanation rate was measured under different spectral regions using a solar simulator. Under 3.2 suns of intensity, the nanowire system activated the Sabatier reaction process at a rate of 0.99 µmol g^{-1} h^{-1}. Another significant result of the investigation is that photochemical activation can be achieved by using near-infrared photons. This suggests implementing an entire tandem hydrogen structure, one in which the ultraviolet-visible part of the spectrum could be used to produce H_2 that could be further used to reduce CO_2. Even though good results were obtained with the addition of ruthenium, replacing it with a less expensive catalyst, such as Ni, would be desired in the future.

Many other works have reported that the morphology of the nanowires can enhance the photo/electrocatalytic performance as well as photoanode platforms (Dasgupta *et al.,* 2013; C. Liu *et al.,* 2014; Lv *et al.,* 2015; P. Yang *et al.,* 2010).

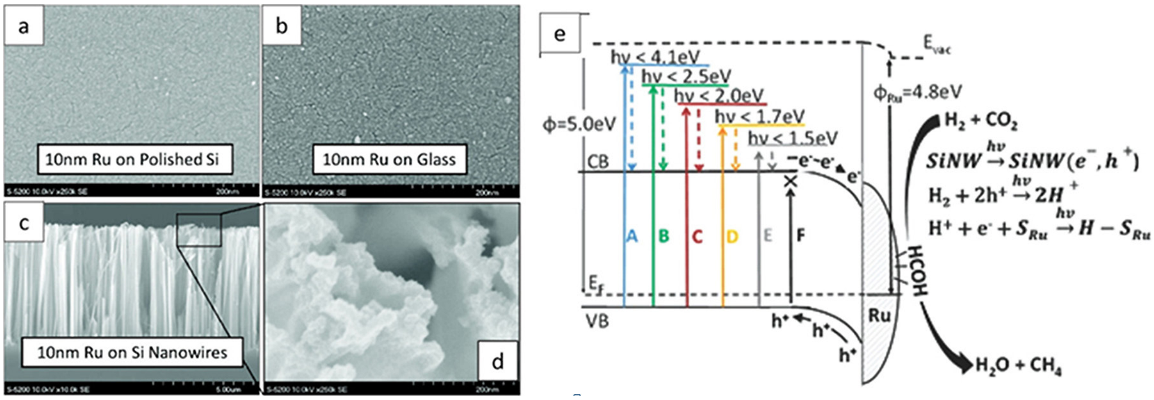

Figure 3. SEM micrograph showing 10 nm Ru coating over a) Si substrate, b) glass, c and d) Si NWs, e) Energy band diagram at the interface of SiNW and Ru(O'Brien *et al.,* 2014). Copyrights Wiley 2014.

Silicon nanowires provide a large surface area for co-catalyst loading and electrochemical reaction sites while at the same time leading to enhanced charge collection efficiency, especially for indirect band gap semiconductors with short minority carrier diffusion lengths.For example, the work of Ma *et al.* (2021) reports the use of a selective platform for photoelectrocatalytic CO_2 reduction using Si NWs with Ni-In bimetallic catalysts. The results of the study show that the nanostructure of the photocathode not only allows reducing the reflectance of the incident light but also enhances the transport of the charges achieving a 5-fold increase in performance with respect to flat materials. Furthermore, the addition of Ni-In co-catalyzing nanoparticles improves the selectivity toward the platform formate, reducing the parasitic hydrogen generation in the reaction.

A summary of other Si-based materials applied to the catalytic reduction of CO_2 is presented in Table 3.For this reason, silicon outstands as an interesting candidate regarding energy harvesting and photocatalytic applications.

Conclusions and future challenges

As stated in this work, heterogeneous catalytic reactions for reducing CO_2 into desirable alcohols and hydrocarbons are of great importance. This is due to the pressing need to adopt carbon recycling procedures to mitigate the anthropogenic impact on the carbon cycle. For this reason, many compounds have been implemented in the electro/photocatalysis reduction of this polluting gas.

Parameters such as pH, temperature, and pressure have been demonstrated to affect catalytic performance. Furthermore, developing processes that allowcontrol over the morphological featuresof catalytic platforms also stands out asversatile strategies to improve the performance of electro/photocatalyst materials.

Cu, SnS_2, TiO_2, CO, among other nanostructured-based platforms,have reported improved CO_2 reduction yields. These enhancements are commonly attributed to an increase in surface area (surface availability), defect density, active site concentration, and improvement in charge separation

Photocatalyst	Enhancement	Synthesis	Light/Electric source	Reductant	Products	Yield	Ref
SiC powders	Pb, Cu, Pd, Fe, and Pt-loaded	Solvent Evaporation	500 W Xe lamp	H_2O	CH_2O_2, CH_2O CH_4O, C_2H_4O, C_2H_6O	~0.033 73 μmol g^{-1}	(Yamamura *et al.*, 1988)
Ti/ Mesoporous silica thin film	Doping / nanostructuration	Solvent Evaporation	100 W Hg lamp	H_2O	$CH_{4,}$ CH_4O	CH_4 7 μmol g^{-1} h^{-1} CH_4O 2 μmol g^{-1} h^{-1}	(Shioya *et al.*, 2003)
Hydrogen-terminated p-type silicon	Sensitization with bipyridine ligands	—	Potentiostat/ galvanostat	0.1 M TBAH	CO	FE 97%	(Kumar *et al.*, 2010)
Ru/Si Nanowires	Nanocomposite	MaCE Sputtering	3.2 suns Xe lamp	CO_2: H_2 ratio of 4:1	CH_4	Dark 0.51 μmol g^{-1} h^{-1} Light 0.99 μmol g^{-1} h^{-1}	(O'Brien *et al.*, 2014)
Hydrogen-terminated silicon nanowires (SiNWs-H)	Mn-based homogeneous molecular catalysts / nanostructuration	MaCE	Cyclic voltammetry	CH_3CN+5% V/V H_2O	CO	Energy conversion 2.1-3.0	(Torralba -Penalver *et al.*, 2015)
SiNWs/$In_2O_{3-x}(OH)_y$ NPs	Nanostructuration/ coupling	MaCE	300 W Xe lamp	1:1 mixture H_2:CO_2 at a pressure of 2 atm	CO	22.0 μmol•g^{-1}•h^{-1}	(Hoch *et al.*, 2016)
SiNWs/Co(II) molecular catalyst	Nanostructuration/ coupling	Not mentioned	Cyclic voltammetry/300 W Xe lamp	CO_2 99.999%	CO	FE69%	(D. He *et al.*, 2016)
SiC granular material	–	Acquired from Saint-Gobain	Laser radiation of 355 nm	CO_2 gas (99.99%)	CH_4O	150 μmol g^{-1}	(Gondal *et al.*, 2012)
Silicon nanocrystals (SiNCs)	Nanostructuration	High-energy ball milling	200 W xenon lamp	0.01 M Na_2CO_3	CH_2O	2 μg cm^{-3}	(Peng *et al.*, 2013)
Si/TiO_2 nanospheres	Nanostructuration/ Heterostructure	Hydrothermal method	300 W Xe arc lamp/355 nm pulse laser radiation	CO_2 gas at 50 psi	CH_4	1.0 μmol g^{-1}	(Y. Liu *et al.*, 2014)
Si NWs/Re(I)-NHC	Nanostructuration/ coupling	Not mentioned	Cyclic voltammetry	CO_2	CO	FE 57-53%	(Jin *et al.*, 2016)

TBAH: tetrabutyl ammonium hexafluorophosphate; In2O3-x(OH)y NPs: hydroxylated indium oxide nanoparticles; NHC: N-heterocyclic carbene.

Table 3. Si-based systems used for CO_2 photo/electro reduction.

efficiency. In addition, preferential facets presented in certain types of morphologies, porosity, and size distribution, impact the physicochemical properties of the nanostructured materials and thus affect the selectivity of the electro/photocatalytic CO_2 reduction reactions.

Yet, some of these systems present major drawbacks, such as low chemical stability, difficult reusability, and major production costs. Therefore, obtaining cheap, abundant, and low-toxicity catalytic materials is also interesting. In this aspect, materials based on ZnO and Si are suitable candidates for CO_2 recycling applications. In the case of ZnO, the improvement of its CO_2 reduction performance is mainly based on reducing excitonic recombination losses through efficient charge transport, implementation of co-catalysts, and heterostructure generation. In addition, their photoactivation in the visible by doping and functionalization to modulate adsorption over large surface areas has provenviable strategies to increase catalytic performance.

Finally, metal deposition on silicon-based nanostructured platforms results in local heating, localized plasmonic behavior, and electronic polarity to improve the performance toward CO_2 reduction. Yet, substitution by cheap and abundant metals is still necessary for implementing these systems.

With all this in mind, there are still several challenges toachieving scalable, cost-effective, and stable electro/photocatalysts for CO_2 recycling applications. However, morphological manipulation strategies in synergy with other reported enhancement tactics promise to impact today's sustainability challenges.

Acknowledgments

A.G.M gratefully acknowledges CONACyT Scholarship CVU 860916. A.D. Acknowledges PAPIIT DGAPA Project IA101321 and IA100123. ♦

REFERENCES

Ali, A., Biswas, M. R. U. D., & Oh, W. C. (2018). Novel and simple process for the photocatalytic reduction of CO_2 with ternary Bi_2O_3-graphene-ZnO nanocomposite. *Journal of Materials Science: Materials in Electronics, 29*(12), 10222-10233. https://doi.org/10.1007/s10854-018-9073-5

Basumallick, S. (2020). Electro-reduction of CO_2 onto ZnO-Cu nano composite catalyst. *Applied Nanoscience (Switzerland), 10*(1), 159-163. https://doi.org/10.1007/s13204-019-01080-8

Bocarsly, A. B., Bookbinder, D. C., Dominey, R. N., Lewis, N. S., & Wrighton, M. S. (1980). Photoreduction at Illuminated p-Type Semiconducting Silicon Photoelectrodes. Evidence for Fermi Level Pinning. *Journal of the American Chemical Society, 102*(11), 3683-3688. https://doi.org/10.1021/ja00531a003

Bouras, P., Stathatos, E., & Lianos, P. (2007). Pure versus metal-ion-doped nanocrystalline titania for photocatalysis. *Applied Catalysis B: Environmental, 73*(1-2), 51-59. https://doi.org/10.1016/j.apcatb.2006.06.007

Cai, W., Shi, Y., Zhao, Y., Chen, M., Zhong, Q., & Bu, Y. (2018). The solvent-driven formation of multi-morphological Ag-CeO_2 plasmonic photocatalysts with enhanced visible-light photocatalytic reduction of CO_2. *RSC Advances*, 8(71), 40731-40739. https://doi.org/10.1039/c8ra08938h

Chen, P., Zhang, Y., Zhou, Y., & Dong, F. (2021). Photoelectrocatalytic carbon dioxide reduction: Fundamental, advances and challenges. *Nano Materials Science, 3*(4), 344-367. https://doi.org/10.1016/j.nanoms.2021.05.003

Christopher, P., Xin, H., & Linic, S. (2011). Visible-light-enhanced catalytic oxidation reactions on plasmonic silver nanostructures. *Nature Chemistry, 3*(6), 467-472. https://doi.org/10.1038/nchem.1032

Dasgupta, N. P., Liu, C., Andrews, S., Prinz, F. B., & Yang, P. (2013). Atomic layer deposition of platinum catalysts on nanowire surfaces for photoelectrochemical water reduction. *Journal of the American Chemical Society, 135*(35), 12932-12935. https://doi.org/10.1021/ja405680p

de Brito, J. F., Araujo, A. R., Rajeshwar, K., & Zanoni, M. V. B. (2015). Photoelectrochemical reduction of CO_2 on Cu/Cu_2O films: Product distribution and pH effects. *Chemical Engineering Journal, 264*, 302-309. https://doi.org/10.1016/j.cej.2014.11.081

Deng, H., Xu, F., Cheng, B., Yu, J., & Ho, W. (2020). Photocatalytic CO_2 reduction of C/ZnO nanofibers enhanced by an Ni-NiS cocatalyst. *Nanoscale, 12*(13), 7206-7213. https://doi.org/10.1039/c9nr10451h

Dong, H., Zeng, G., Tang, L., Fan, C., Zhang, C., He, X., & He, Y. (2015). An overview on limitations of TiO$_2$-based particles for photocatalytic degradation of organic pollutants and the corresponding countermeasures. *Water Research, 79,* 128-146. https://doi.org/10.1016/j.watres.2015.04.038

Feng, X., Zou, H., Zheng, R., Wei, W., Wang, R., Zou, W., Lim, G., Hong, J., Duan, L., & Chen, H. (2022). Bi$_2$O$_3$/BiO$_2$ Nanoheterojunction for Highly Efficient Electrocatalytic CO$_2$ Reduction to Formate. *Nano Letters, 22*(4), 1656-1664. https://doi.org/10.1021/acs.nanolett.1c04683

Fox, M. A., & Dulay, M. T. (1993). Heterogeneous Photocatalysis. *Chemical Reviews, 93*(1), 341-357. https://doi.org/10.1021/cr00017a016

Galdámez-Martínez, A., Bai, Y., Santana, G., Sprick, R. S., & Dutt, A. (2020). Photocatalytic hydrogen production performance of 1-D ZnO nanostructures: Role of structural properties. *International Journal of Hydrogen Energy, 45*(xxxx), 1-10. https://doi.org/10.1016/j.ijhydene.2020.08.247

Gao, T., Wen, X., Xie, T., Han, N., Sun, K., Han, L., Wang, H., Zhang, Y., Kuang, Y., & Sun, X. (2019). Morphology effects of bismuth catalysts on electroreduction of carbon dioxide into formate. *Electrochimica Acta,* 305, 388-393. https://doi.org/10.1016/j.electacta.2019.03.066

Gao, Z. H., Wei, K., Wu, T., Dong, J., Jiang, D. E., Sun, S., & Wang, L. S. (2022). A Heteroleptic Gold Hydride Nanocluster for Efficient and Selective Electrocatalytic Reduction of CO$_2$ to CO. *Journal of the American Chemical Society, 144*(12), 5258-5262. https://doi.org/10.1021/jacs.2c00725

Geng, Z., Kong, X., Chen, W., Su, H., Liu, Y., Cai, F., Wang, G., & Zeng, J. (2018). Oxygen Vacancies in ZnO Nanosheets Enhance CO$_2$ Electrochemical Reduction to CO. *Angewandte Chemie - International Edition, 57*(21), 6054-6059. https://doi.org/10.1002/anie.201711255

Ghahramanifard, F., Rouhollahi, A., & Fazlolahzadeh, O. (2018). Synthesis of n-type Cu-doped ZnO Nanorods onto FTO by Electrodeposition Method and Study its Electrocatalytic Properties toward CO$_2$ Reduction. *Analytical & Bioanalytical Electrochemistry, 10*(3), 362-371.

Gondal, M. A., Ali, M., Chang, X. F., Shen, K., Xu, Q. Y., & Yamani, Z. H. (2012). Pulsed laser-induced photocatalytic reduction of greenhouse gas CO$_2$ into methanol: A value-added hydrocarbon product over SiC. *Journal of Environmental Science and Health - Part A Toxic/Hazardous Substances and Environmental Engineering, 47*(11), 1571-1576. https://doi.org/10.1080/10934529.2012.680419

Guo, F., Yang, S., Liu, Y., Wang, P., Huang, J., & Sun, W. Y. (2019). Size Engineering of Metal-Organic Framework MIL-101(Cr)-Ag Hybrids for Photocatalytic CO$_2$ Reduction [Research-article]. *ACS Catalysis, 9*(9), 8464-8470. https://doi.org/10.1021/acscatal.9b02126

Guo, Q., Zhang, Q., Wang, H., Liu, Z., & Zhao, Z. (2017). Unraveling the role of surface property in the photoreduction performance of CO$_2$ and H$_2$O catalyzed by the modified ZnO. *Molecular Catalysis, 436,* 19-28. https://doi.org/10.1016/j.mcat.2017.04.014

Habisreutinger, S. N., Schmidt-Mende, L., & Stolarczyk, J. K. (2013). Photocatalytic reduction of CO$_2$ on TiO$_2$ and other semiconductors. *Angewandte Chemie - International Edition,* 52(29), 7372-7408. https://doi.org/10.1002/anie.201207199

Han, N., Ding, P., He, L., Li, Y., & Li, Y. (2020). Promises of Main Group Metal-Based Nanostructured Materials for Electrochemical CO$_2$ Reduction to Formate. *Advanced Energy Materials, 10*(11), 1-19. https://doi.org/10.1002/aenm.201902338

He, D., Jin, T., Li, W., Pantovich, S., Wang, D., & Li, G. (2016). Photoelectrochemical CO$_2$ Reduction by a Molecular Cobalt (II) Catalyst on Planar and Nanostructured Si Surfaces. *Chemistry - A European Journal, 22*(37), 13064-13067.

He, J., Johnson, N. J. J., Huang, A., & Berlinguette, C. P. (2018). Electrocatalytic Alloys for CO$_2$ Reduction. *ChemSusChem, 11*(1), 48-57. https://doi.org/10.1002/cssc.201701825

Hoch, L. B., Brien, P. G. O., Jelle, A., Sandhel, A., Perovic, D. D., Mims, C. A., & Ozin, A. (2016). *Nanostructured Indium Oxide Coated Silicon Nanowire Arrays: A Hybrid Photothermal/ Photochemical Approach to Solar Fuels.* https://doi.org/10.1021/acsnano.6b05416

Inoue, T., Fujishima, A., Konishi, S., & Honda, K. (1979). Photoelectrocatalytic reduction of carbon dioxide in aqueous suspensions of semiconductor powders. In *Nature* (Vol. 277, Issue 5698, pp. 637-638). https://doi.org/10.1038/277637a0

Iqbal, M., Wang, Y., Hu, H., He, M., Hassan Shah, A., Lin, L., Li, P., Shao, K., Reda Woldu, A., & He, T. (2018). Cu$_2$O-tipped ZnO nanorods with enhanced photoelectrochemical performance for CO_2 photoreduction. *Applied Surface Science, 443,* 209-216. https://doi.org/10.1016/j.apsusc.2018.02.162

Jayah, N. A., Yahaya, H., Mahmood, M. R., Terasako, T., Yasui, K., & Hashim, A. M. (2015). High electron mobility and low carrier concentration of hydrothermally grown ZnO thin films on seeded a-plane sapphire at low temperature. *Nanoscale Research Letters, 10*(1), 1-10. https://doi.org/10.1186/s11671-014-0715-0

Jiang, K., Wang, H., Cai, W. Bin, & Wang, H. (2017). Li Electrochemical Tuning of Metal Oxide for Highly Selective CO_2 Reduction. *ACS Nano, 11*(6), 6451-6458. https://doi.org/10.1021/acsnano.7b03029

Jiang, X., Cai, F., Gao, D., Dong, J., Miao, S., Wang, G., & Bao, X. (2016). Electrocatalytic reduction of carbon dioxide over reduced nanoporous zinc oxide. *Electrochemistry Communications, 68,* 67-70. https://doi.org/10.1016/j.elecom.2016.05.003

Jin, T., He, D., Li, W., Iii, J. S., & Pantovich, S. A. (2016). CO_2 reduction with Re (I)-NHC compounds: driving selective catalysis with a silicon nanowire. *Chemical Communications, 52,* 14258-14261. https://doi.org/10.1039/C6CC08240H

Kočí, K., Obalová, L., Matějová, L., Plachá, D., Lacný, Z., Jirkovský, J., & Šolcová, O. (2009). Effect of TiO_2 particle size on the photocatalytic reduction of CO_2. *Applied Catalysis B: Environmental, 89*(3-4), 494-502. https://doi.org/10.1016/j.apcatb.2009.01.010

Kočí, K., Praus, P., Edelmannová, M., Ambrožová, N., Troppová, I., Fridrichová, D., Słowik, G., & Ryczkowski, J. (2017). Photocatalytic reduction of CO_2 over CdS, ZnS and core/shell CdS/ZnS nanoparticles deposited on montmorillonite. *Journal of Nanoscience and Nanotechnology, 17*(6), 4041-4047. https://doi.org/10.1166/jnn.2017.13093

Kumar, B., Smieja, J. M., & Kubiak, C. P. (2010). Photoreduction of CO_2 on p-type silicon using Re(bipy-Bu t)(CO)3Cl: Photovoltages exceeding 600 mV for the selective reduction of CO_2 to CO. *Journal of Physical Chemistry C, 114*(33), 14220-14223. https://doi.org/10.1021/jp105171b

Li, D., Kassymova, M., Cai, X., Zang, S. Q., & Jiang, H. L. (2020). Photocatalytic CO_2 reduction over metal-organic framework-based materials. *Coordination Chemistry Reviews*, 412, 213262. https://doi.org/10.1016/j.ccr.2020.213262

Li, G., Sun, Y., Sun, S., Chen, W., Zheng, J., Chen, F., Sun, Z., & Sun, W. (2020). The effects of morphologies on photoreduction of carbon dioxide to gaseous fuel over tin disulfide under visible light irradiation. *Advanced Powder Technology, 31*(6), 2505-2512. https://doi.org/10.1016/j.apt.2020.04.014

Li, H., Lei, Y., Huang, Y., Fang, Y., Xu, Y., Zhu, L., & Li, X. (2011). Photocatalytic reduction of carbon dioxide to methanol by Cu 2O/SiC nanocrystallite under visible light irradiation. *Journal of Natural Gas Chemistry, 20*(2), 145-150. https://doi.org/10.1016/S1003-9953(10)60166-1

Li, M., Zhang, S., Li, L., Han, J., Zhu, X., Ge, Q., & Wang, H. (2020). Construction of Highly Active and Selective Polydopamine Modified Hollow ZnO/Co_3O_4p-n Heterojunction Catalyst for Photocatalytic CO_2 Reduction. *ACS Sustainable Chemistry and Engineering, 8*(30), 11465-11476. https://doi.org/10.1021/acssuschemeng.0c04829

Li, N., Chen, X., Wang, J., Liang, X., Ma, L., Jing, X., Chen, D. L., & Li, Z. (2022). ZnSe Nanorods-$CsSnCl_3$ Perovskite Heterojunction Composite for Photocatalytic CO_2 Reduction. *ACS Nano, 16*(2), 3332-3340. https://doi.org/10.1021/acsnano.1c11442

Li, P., Zhu, S., Hu, H., Guo, L., & He, T. (2019). Influence of defects in porous ZnO nanoplates on CO_2 photoreduction. *Catalysis Today, 335,* 300-305. https://doi.org/10.1016/j.cattod.2018.11.068

Li, Z., He, D., Yan, X., Dai, S., Younan, S., Ke, Z., Pan, X., Xiao, X., Wu, H., & Gu, J. (2020). Size-Dependent Nickel-Based Electrocatalysts for Selective CO_2 Reduction. *Angewandte Chemie - International Edition, 59*(42), 18572-18577. https://doi.org/10.1002/anie.202000318

Liao, F., Fan, X., Shi, H., Li, Q., Ma, M., Zhu, W., Lin, H., Li, Y., & Shao, M. (2022). Boosting electrocatalytic selectivity in carbon dioxide reduction: The fundamental role of dispersing gold nanoparticles on silicon nanowires. *Chinese Chemical Letters, 33*(9), 4380-4384. https://doi.org/10.1016/j.cclet.2021.12.034

Liao, Y., Hu, Z., Gu, Q., & Xue, C. (2015). Amine-functionalized ZnO nanosheets for efficient CO_2 capture and photoreduction. *Molecules, 20*(10), 18847-18855. https://doi.org/10.3390/molecules201018847

Lin, L.-Y. Y., Kavadiya, S., Karakocak, B. B., Nie, Y., Raliya, R., Wang, S. T., Berezin, M. Y., & Biswas, P. (2018). ZnO_{1-x}/carbon dots composite hollow spheres: Facile aerosol synthesis and superior CO_2 photoreduction under UV, visible and near-infrared irradiation. *Applied Catalysis B: Environmental, 230,* 36-48. https://doi.org/10.1016/j.apcatb.2018.02.018

Liu, C., Dasgupta, N. P., & Yang, P. (2014). Semiconductor nanowires for artificial photosynthesis. *Chemistry of Materials, 26*(1), 415-422. https://doi.org/10.1021/cm4023198

Liu, L., & Jin, F. (2017). Hybrid ZnO nanorod arrays@graphene through a facile room-temperature bipolar solution route towards advanced CO_2 photocatalytic reduction properties. *Ceramics International, 43*(1), 860-865. https://doi.org/10.1016/j.ceramint.2016.09.112

Liu, X., Ye, L., Liu, S., Li, Y., & Ji, X. (2016). Photocatalytic Reduction of CO_2 by ZnO Micro/nanomaterials with Different Morphologies and Ratios of {0001} Facets. *Scientific Reports, 6*(December), 38474. https://doi.org/10.1038/srep38474

Liu, Y., Ji, G., Dastageer, M. A., Zhu, L., Wang, J., Zhang, B., Chang, X., & Gondal, M. A. (2014). Highly-active direct Z-scheme Si/TiO_2 photocatalyst for boosted CO_2 reduction into value-added methanol. *RSC Advances, 4*(100), 56961-56969. https://doi.org/10.1039/c4ra10670a

Loutzenhiser, P. G., Elena Gálvez, M., Hischier, I., Graf, A., & Steinfeld, A. (2010). CO_2 splitting in an aerosol flow reactor via the two-step Zn/ZnO solar thermochemical cycle. *Chemical Engineering Science, 65*(5), 1855-1864. https://doi.org/10.1016/j.ces.2009.11.025

Lv, C., Chen, Z., Chen, Z., Zhang, B., Qin, Y., Huang, Z., & Zhang, C. (2015). Silicon nanowires loaded with iron phosphide for effective solar-driven hydrogen production. *Journal of Materials Chemistry A, 3*(34), 17669-17675. https://doi.org/10.1039/c5ta03438h

Ma, W., Xie, M., Xie, S., Wei, L., Cai, Y., Zhang, Q., & Wang, Y. (2021). Nickel and indium core-shell co-catalysts loaded silicon nanowire arrays for efficient photoelectrocatalytic reduction of CO_2 to formate. *Journal of Energy Chemistry, 54,* 422-428. https://doi.org/10.1016/j.jechem.2020.06.023

Merino-Garcia, I., Albo, J., Solla-Gullón, J., Montiel, V., & Irabien, A. (2019). Cu oxide/ZnO-based surfaces for a selective ethylene production from gas-phase CO_2 electroconversion. *Journal of CO_2 Utilization, 31*(November 2018), 135-142. https://doi.org/10.1016/j.jcou.2019.03.002

Miao, Z., Liu, W., Zhao, Y., Wang, F., Meng, J., Liang, M., Wu, X., Zhao, J., Zhuo, S., & Zhou, J. (2020). Zn-Modified Co@N-C composites with adjusted Co particle size as catalysts for the efficient electroreduction of CO_2. *Catalysis Science and Technology, 10*(4), 967-977. https://doi.org/10.1039/c9cy02203a

Núñez, J., De La Peña O'Shea, V. A., Jana, P., Coronado, J. M., & Serrano, D. P. (2013). Effect of copper on the performance of ZnO and $ZnO_{1-x}N_x$ oxides as CO_2 photoreduction catalysts. *Catalysis Today, 209*, 21-27. https://doi.org/10.1016/j.cattod.2012.12.022

O'Brien, P. G., Sandhel, A., Wood, T. E., Jelle, A. A., Hoch, L. B., Perovic, D. D., Mims, C. A., & Ozin, G. A. (2014). Photomethanation of gaseous CO_2 over ru/silicon nanowire catalysts with visible and near-infrared photons. *Advanced Science, 1*(1), 1-7. https://doi.org/10.1002/advs.201400001

Peng, F., Wang, J., Ge, G., He, T., Cao, L., He, Y., Ma, H., & Sun, S. (2013). Photochemical reduction of CO_2 catalyzed by silicon nanocrystals produced by high energy ball milling. *Materials Letters, 92*, 65-67. https://doi.org/10.1016/j.matlet.2012.10.059

Qiao, Y., Lai, W., Huang, K., Yu, T., Wang, Q., Gao, L., Yang, Z., Ma, Z., Sun, T., Liu, M., Lian, C., & Huang, H. (2022). Engineering the Local Microenvironment over Bi Nanosheets for Highly Selective Electrocatalytic Conversion of CO_2 to HCOOH in Strong Acid. *ACS Catalysis, 12*(4), 2357-2364. https://doi.org/10.1021/acscatal.1c05135

Rong, W., Zou, H., Zang, W., Xi, S., Wei, S., Long, B., Hu, J., Ji, Y., & Duan, L. (2021). Size-Dependent Activity and Selectivity of Atomic-Level Copper Nanoclusters during CO/CO_2 Electroreduction. *Angewandte Chemie - International Edition, 60*(1), 466-472. https://doi.org/10.1002/anie.202011836

Scirè, S., Crisafulli, C., Maggiore, R., Minicò, S., & Galvagno, S. (1998). Influence of the support on CO_2 methanation over Ru catalysts: An FT-IR study. *Catalysis Letters, 51*(1), 41-45. https://doi.org/10.1023/A:1019028816154

Shehzad, N., Tahir, M., Johari, K., Murugesan, T., & Hussain, M. (2018). A critical review on TiO_2 based photocatalytic CO_2 reduction system: Strategies to improve efficiency. *Journal of CO_2 Utilization, 26*(November 2017), 98-122. https://doi.org/10.1016/j.jcou.2018.04.026

Shioya, Y., Ikeue, K., Ogawa, M., & Anpo, M. (2003). Synthesis of transparent Ti-containing mesoporous silica thin film materials and their unique photocatalytic activity for the reduction of CO_2 with H_2O. *Applied Catalysis A: General, 254*(2), 251-259. https://doi.org/10.1016/S0926-860X(03)00487-3

Torralba-Penalver, E., Luo, Y., Compain, J.-D., Chardon-Noblat, S., & Fabre, B. (2015). Selective Catalytic Electroreduction of CO_2 at Silicon Nanowires (SiNWs) Photocathodes Using Non-Noble Metal-Based Manganese Carbonyl Bipyridyl Molecular Catalysts in Solution and Grafted onto SiNWs. *ACS Catalysis, 5*(10), 6138-6147. https://doi.org/10.1021/acscatal.5b01546

Wang, C., Thompson, R. L., Ohodnicki, P., Baltrus, J., & Matranga, C. (2011). Size-dependent photocatalytic reduction of CO_2 with PbS quantum dot sensitized TiO_2 heterostructured photocatalysts. *Journal of Materials Chemistry, 21*(35), 13452-13457. https://doi.org/10.1039/c1jm12367j

Wang, J., Han, B., Nie, R., Xu, Y., Yu, X., Dong, Y., Wang, J., & Jing, H. (2018). Photoelectrocatalytic Reduction of CO_2 to Chemicals via ZnO@Nickel Foam: Controlling C-C Coupling by Ligand or Morphology. *Topics in Catalysis, 61*(15-17), 1563-1573. https://doi.org/10.1007/s11244-018-1018-y

Wang, W.-N., Soulis, J., Yang, Y. J., & Biswas, P. (2014). Comparison of CO_2 Photoreduction Systems: A Review. *Aerosol and Air Quality Research, 14*(2), 533-549. https://doi.org/10.4209/aaqr.2013.09.0283

Wang, X., Li, Q., Zhou, C., Cao, Z., & Zhang, R. (2019). ZnO rod/reduced graphene oxide sensitized by α-Fe_2O_3 nanoparticles for effective visible-light photoreduction of CO_2. *Journal of Colloid and Interface Science, 554*, 335-343. https://doi.org/10.1016/j.jcis.2019.07.014

Wang, Y., Ren, B., Zhen Ou, J., Xu, K., Yang, C., Li, Y., & Zhang, H. (2021). Engineering two-dimensional metal oxides and chalcogenides for enhanced electro- and photocatalysis. *Science Bulletin, 66*(12), 1228-1252. https://doi.org/10.1016/j.scib.2021.02.007

Wang, Y., Zhu, Y., & Niu, C. (2020). Surface and length effects for aqueous electrochemical reduction of CO_2 as studied over copper nanowire arrays. *Journal of Physics and Chemistry of Solids, 144*(January), 109507. https://doi.org/10.1016/j.jpcs.2020.109507

Watanabe, M. (1992). Photosynthesis of methanol and methane from CO_2 and H_2O molecules on a ZnO surface. *Surface Science*, *279*(3), 236-242. https://doi.org/10.1016/0039-6028(92)90546-I

Wei, B., Xiong, Y., Zhang, Z., Hao, J., Li, L., & Shi, W. (2021). Efficient electrocatalytic reduction of CO_2 to HCOOH by bimetallic In-Cu nanoparticles with controlled growth facet. *Applied Catalysis B: Environmental, 283,* 119646. https://doi.org/10.1016/j.apcatb.2020.119646

Woldu, A. R., Huang, Z., Zhao, P., Hu, L., & Astruc, D. (2022). Electrochemical CO_2 reduction (CO_2RR) to multi-carbon products over copper-based catalysts. *Coordination Chemistry Reviews, 454*, 214340. https://doi.org/10.1016/j.ccr.2021.214340

Wong, A. P. Y., Sun, W., Qian, C., Jelle, A. A., Jia, J., Zheng, Z., Dong, Y., & Ozin, G. A. (2017). Tailoring CO_2 Reduction with Doped Silicon Nanocrystals. *Advanced Sustainable Systems, 1*(11), 1-7. https://doi.org/10.1002/adsu.201700118

Xu, T., Hu, J., Yang, Y., Que, W., Yin, X., Wu, H., & Chen, L. (2018). Solid-state synthesis of ZnO nanorods coupled with reduced graphene oxide for photocatalytic application. *Journal of Materials Science: Materials in Electronics, 29*(6), 4888-4894. https://doi.org/10.1007/s10854-017-8447-4

Xuan, X., Tu, S., Yu, H., Du, X., Zhao, Y., He, J., Dong, H., Zhang, X., & Huang, H. (2019). Size-dependent selectivity and activity of CO_2 photoreduction over black nano-titanias grown on dendritic porous silica particles. *Applied Catalysis B: Environmental, 255*(May), 117768. https://doi.org/10.1016/j.apcatb.2019.117768

Yamamura, S., Kojima, H., Iyoda, J., & Kawai, W. (1988). Photocatalytic reduction of carbon dioxide with metal-loaded SiC powders. *Journal of Electroanalytical Chemistry, 247*(1-2), 333-337. https://doi.org/10.1016/0022-0728(88)80154-2

Yang, G., Qiu, P., Xiong, J., Zhu, X., & Cheng, G. (2022). Facilely anchoring Cu2O nanoparticles on mesoporous TiO_2 nanorods for enhanced photocatalytic CO_2 reduction through efficient charge transfer. *Chinese Chemical Letters, 33*(8), 3709-3712. https://doi.org/10.1016/j.cclet.2021.10.047

Yang, P., Yan, R., & Fardy, M. (2010). Semiconductor nanowire: Whats Next? *Nano Letters, 10*(5), 1529-1536. https://doi.org/10.1021/nl100665r

Yin, H. Y., Zheng, Y. F., & Song, X. C. (2019). Synthesis and enhanced visible light photocatalytic

CO$_2$ reduction of $BiPO_4$-$BiOBr_xI_{1-x}$ p-n heterojunctions with adjustable energy band. *RSC Advances*, *9*(20), 11005-11012. https://doi.org/10.1039/c9ra01416k

Zhang, L., Li, N., Jiu, H., Qi, G., & Huang, Y. (2015). ZnO-reduced graphene oxide nanocomposites as efficient photocatalysts for photocatalytic reduction of CO$_2$. *Ceramics International*, *41*(5), 6256-6262. https://doi.org/10.1016/j.ceramint.2015.01.044

Zhang, L., Zhao, Z. J., & Gong, J. (2017). Nanostructured Materials for Heterogeneous Electrocatalytic CO$_2$ Reduction and their Related Reaction Mechanisms. *Angewandte Chemie - International Edition*, *56*(38), 11326-11353. https://doi.org/10.1002/anie.201612214

Zhang, X., Wang, P., Lv, X., Niu, X., Lin, X., Zhong, S., Wang, D., Lin, H., Chen, J., & Bai, S. (2022). Stacking Engineering of Semiconductor Heterojunctions on Hollow Carbon Spheres for Boosting Photocatalytic CO$_2$ Reduction. *ACS Catalysis*, *12*(4), 2569-2580. https://doi.org/10.1021/acscatal.1c05401

Zhao, Z., Fan, J., Wang, J., & Li, R. (2012). Effect of heating temperature on photocatalytic reduction of CO$_2$ by N-TiO$_2$ nanotube catalyst. *Catalysis Communications*, *21*, 32-37. https://doi.org/10.1016/j.catcom.2012.01.022

Zheng, Y., Yin, X., & Zhang, S. (2018). Activity Enhancement in Photocatalytic Reduction of CO$_2$ over Nano-ZnO Anchored on Graphene. *Water, Air, and Soil Pollution*, *229*(8). https://doi.org/10.1007/s11270-018-3877-z

Zhu, W., Zhang, L., Yang, P., Chang, X., Dong, H., Li, A., Hu, C., Huang, Z., Zhao, Z. J., & Gong, J. (2018). Morphological and Compositional Design of Pd-Cu Bimetallic Nanocatalysts with Controllable Product Selectivity toward CO$_2$ Electroreduction. *Small*, *14*(7), 1-7. https://doi.org/10.1002/smll.201703314

* * *